Steel and Composite Structures, *Vol*. *23*, *No*. *3* (*2017*) *351-362*
DOI: https://doi.org/10.12989/scs.2017.23.3.351

Experimental investigation of longitudinal shear behavior for composite floor slab

Marcela N. Kataoka *, Juliana T. Friedrich [a] and Ana Lúcia H.C. El Debs [b]

University of São Paulo, *Engineering School of São Carlos*, *Structural Department*,
Av. *Trabalhador Saocarlense*, *nº 400*, *CEP*: *13566-580*, *São Carlos*, *SP*, *Brazil*

(*Received June 11*, *2015*, *Revised December 05*, *2016*, *Accepted January 16*, *2017*)

Abstract. This paper presents an experimental study on the behavior of composite floor slab comprised by a new steel sheet and concrete slab. The strength of composite slabs depends mainly on the strength of the connection between the steel sheet and concrete, which is denoted by longitudinal shear strength. The composite slabs have three main failures modes, failure by bending, vertical shear failure and longitudinal shear failure. These modes are based on the load *versus* deflection curves that are obtained in bending tests. The longitudinal shear failure is brittle due to the mechanical connection was not capable of transferring the shear force until the failure by bending occurs. The vertical shear failure is observed in slabs with short span, large heights and high concentrated loads subjected near the supports. In order to analyze the behavior of the composite slab with a new steel sheet, six bending tests were undertaken aiming to provide information on their longitudinal shear strength, and to assess the failure mechanisms of the proposed connections. Two groups of slabs were tested, one with 3000 mm in length and other with 1500 mm in length. The tested composite slabs showed satisfactory composite behavior and longitudinal shear resistance, as good as well, the analysis confirmed that the developed sheet is suitable for use in composite structures without damage to the global behavior.

Keywords: composite structures; slim-floor; composite slab; longitudinal shear; bending test

1. Introduction

The composite elements are constituted by two or more elements of different materials working together. In the case of steel and concrete, there is always a steel profile (welded, rolled or folded) combined with a concrete element (in general reinforced concrete) in order to use the advantages of each material.

The concrete and the steel are the worldwide usual materials that have advantages and disadvantages well known by professionals from this field. However, there are still important issues to be studied on their behavior. The goal of composite construction is taking the advantage and minimizes the disadvantages of each material. The usual composite floor consists of composite beam, slim-floor and shear connectors that ensure the interaction between elements.

Taking this concept into consideration, the shallow floor is a type of composite floor, which has the slab supported on the bottom flange of the steel beam; furthermore, the height of the floor is reduced. The shallow floor allows several configurations of beams and slabs. The cross section of the beams can be like "I", box, hat and others. The slab can be precast (hollow core slab), slim- floor and reinforced concrete.

Some advantages are presented by the shallow floor when it is compared to the usual composite floor (slim floor). The main advantage is the reduction of the height and the smooth appearance without the presence of the beams that meets the architectural and urban requirements. Research has been studying shear connections and flexural resistances of the shallow floor beams in order to provide more information about their behavior, such as Huo and D,Mello (2013) and Chen *et al*. (2015), respectively. The fire protection is also a characteristic of the shallow floor, besides to be an economical solution to reduce costs with workmanship and to provide shorter execution time.

Much previous work has been directed towards composite elements. In the research of Marimuthu *et al*. (2007), the composite behavior between steel sheet and reinforced concrete slab was study. According to the analysis, there are three stages in the structural action during the construction of composite slabs. In the first stage, the steel sheet must support the weight of the cast onsite concrete. When the slab and the steel sheet start working together to support the loading subjected to the structure, the second stage is presented. Finally, the ultimate stage is characterized by the joint action with the beam through the shear connectors.

It is known that the composite slabs subjected to bending can present three main failure modes: failure by bending (Section 1-1); vertical shear failure (Section 2-2), and longitudinal shear failure (Section 3-3), as shown in Fig. 1.

*Corresponding author, Ph.D.,
E-mail: kataoka@sc.usp.br
[a] Student, E-mail: juliana@francaeassociados.com.br
[b] Professor, E-mail: analucia@sc.usp.br

ISSN: 1229-9367 (Print), 1598-6233 (Online)

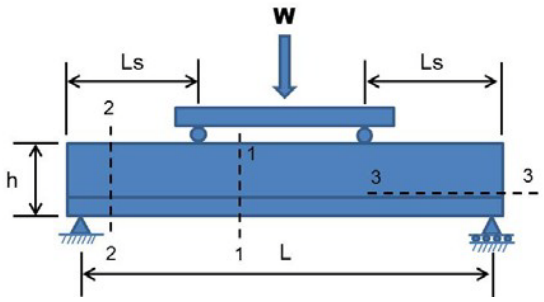

Fig. 1 Failure modes of the composite slabs (Johnson 1994)

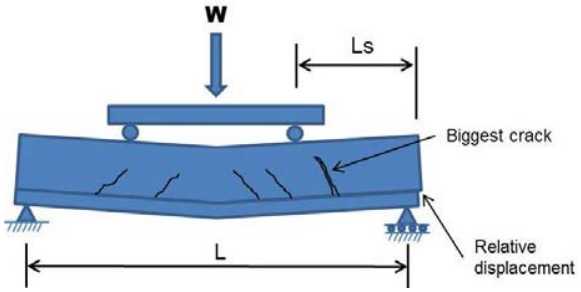

Fig. 2 Failure mode 3 by longitudinal shear

The failure by bending (mode 1) is observed when there is complete interaction in the interface between concrete and steel sheet. This type of failure usually occurs in slabs with wide spans and small heights. The prevention of such failure is easy; reinforcement in the concrete can be done as described in Easterling and Young (1992). However, the failure by bending is not the dominant criterion for sizing due to the interaction between steel and concrete is usually partial and the length of the slab is always limited by serviceability limit state. The Brazilian Code ABNT NBR 8800 (2008) addresses only the design of composite slabs with full interaction.

According to Shen (2001), to the failure mode 2 be predominant, the slab must have short span, and large heights and be subjected to high loads concentrated near the supports. This type of failure is not common. The effect is ignored in the design. The third failure mode, which is the failure by longitudinal shear or commonly known as failure of steel-concrete interface by shear, is more common in composite slabs subjected to vertical loads. This is characterized by the development of a diagonal crack near the concentrated load, followed by a slippage between steel sheet and concrete. Fig. 2 illustrates failure mode 3.

The resistance and behavior of the composite slabs depend on several important factors such as the devices of shear transfer, the thickness of the steel sheet and the thickness of the slab. The devices of shear transfer in steel sheet consist of a combination of dents or embossments in their surface and anchoring devices.

Other aspects that have influence in the performance of the slab are the surface of the steel sheet, the steel strength and density, the strength and age of the concrete. Moreover, Seleim and Schuster (1985) reported that the rate of reinforcement and the compressive strength of concrete have significant influence on the shear strength of the slab interface, but the thickness of the steel sheet is a governing parameter. Other studies also confirm that the compressive strength of concrete does not affect significantly the performance of the slab as Daniels and Crisinel (1988). According to some researchers, the shrinkage of the composite slabs should also be considered in predicting the deformation. Al-Deen *et al*. (2015) carried out long-term tests, where samples were maintained in a simply-supported configuration subjected to their own self-weight, creep and shrinkage for four months. One of the conclusions was that the shrinkage profile of the composite specimens presented larger deflections than the reinforced concrete samples.

The shear strength of the interface between steel sheet and concrete can be divided into three components: chemical bond, friction and mechanical interlock. As explained by Abdullah (2004), the chemical bond is the result of natural adhesion of the cement paste with steel sheet. This adhesion presents a shear strength, which prevents the slippage at the interface between steel sheet and concrete. When that adherence is broken, the slippage begins and the strength of the interface is reduced to zero without the possibility to recover it. The friction strength is a result of the application of normal loads on the slab. That loads are perpendicular to the concrete-steel interface. The joint action of the concrete and steel elements depends on a proper transfer of longitudinal loads between these two elements. This joint action allows the sheet acts as tensile reinforcement when the slab is subjected to bending. In addition to the longitudinal shear loads, the bending also leads to a vertical separation between steel and concrete. In order to prevent the separation, the profile sheet is designed to resist the vertical separation and to transfer the longitudinal shear loads.

The vertical separation is avoided by appropriate trapezoidal cross section and also by dents stamped in profile surface.

In Kim and Jeong (2010), perfobond ribs were welded in the steel sheet in order to develop a composite deck slab for girder bridges that spans longer but weighs less than the conventional reinforced concrete (RC) deck slab. The longitudinal shear capacity of the deck proposed by Kim and Jeong (2010) was estimated by using an empirical m–km–k method and the estimated longitudinal shear resistance was approximately two times greater than the required longitudinal shear strength.

In Vainiünas *et al*. (2006) was also studied the longitudinal shear strength between steel sheet and concrete slab. The results of their research allowed concluding that the strength of the slab mainly depends on the strength of the interface between steel sheet and concrete. In order to evaluate the strength and stiffness of the interface in composite slabs, the research proposed a method of analysis of longitudinal shear. According to the researchers, the experimental and theoretical results of the strength were satisfactory to determine the longitudinal loads.

With the technological advancement and the implementation of Finite Element Method (FEM) in numerical simulations, many studies in this field are being developed to predict the behavior of composite structures without the need of tests. Chen and Shi (2011) studied a model based on the finite element method of nonlinear contact validated by

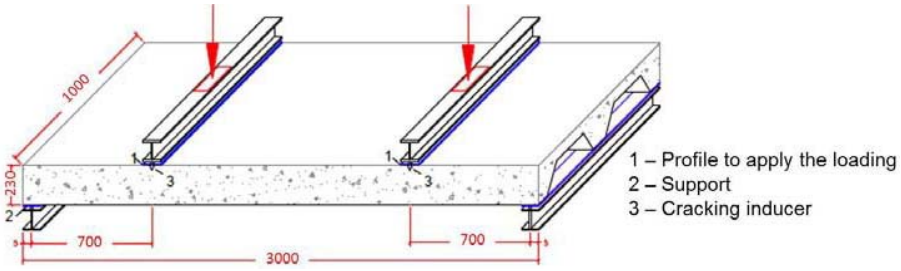

(a) Group 1: models with 3000 mm long (unit: millimeters)

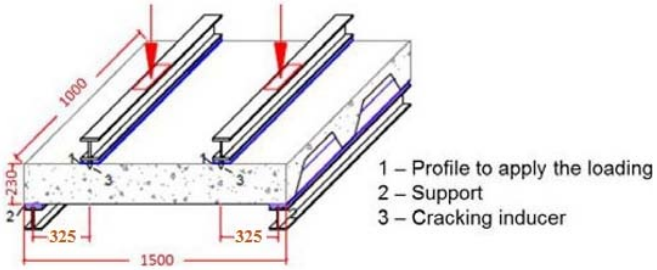

(b) Group 2: models with 1500 mm long (unit: millimeters)

Fig. 3 Test setup

comparison with experimental results. According to the researchers, the comparisons between numerical and experimental results indicate that the finite element model has a good correlation with the experimental values and it is able to predict the strength of composite slabs.

Ferrer *et al*. (2006) conducted a study to understand the mechanisms of the interface steel sheet and concrete, and the dependence of this interface of the geometrical and physical parameters. A 3D finite element models were used to simulate the relative slippage between steel sheet and concrete in tests carried out with reduced-scale models. The following parameters were analyzed: coefficient of friction, depth, geometry, inclination and the distance between dents. The parameters such as inclination of dents and friction had a significant influence on the shear strength of steel and concrete interface.

Generally, the difficulties to evaluate the longitudinal shear strength at interface and the lack of a standardized method of calculation that takes into account this parameter are some reasons for conducting researches. In attempt to analyze the behavior of composite floor, this paper deals with the behavior of shallow floors composed by steel sheet, which was developed specially to this research. The steel sheet was produced according to the predictions observed in previous researches with adequate depth, inclination of dents and trapezoidal geometry. The tests were carried out according to the requirements of EUROCODE 4 (2004), which has been the subject of studies regarding its efficiency, as in Salonikios *et al*. (2012). In this research, the authors verified that the cyclic loading indicated by this standard to break the chemical bond between the steel sheet and concrete would not be enough for such action. In Saravanan *et al*. (2012) it was proved that the application of cyclic loading had no influence on the ultimate strength of the composite slab

Table 1 Groups of slab models

Group	Length (mm)	Model	Monotonic test	Cyclic test
1	3000	Model 1	X	
		Model 2	X	X
		Model 3	X	X
2	1500	Model 4	X	
		Model 5	X	X
		Model 6	X	X

2. Experimental program

The experimental results presented in this paper were obtained in a Master research, Friedrich (2012), performed at University of Sao Paulo and is part of a group, which studies on the behavior of composite structures. The slim floor, the composite beams and slabs and the composite connections were subject of other papers of researchers of this group as De Nardin and El Debs (2009), De Nardin and El Debs (2011), Kataoka and El Debs (2013, 2014, 2015). In addition to experimental analysis, in some papers a numerical analyzes were also conducted to a deep study on the behavior of composite structures.

2.1 Characterization of the models

The experimental program of this research is divided in two main steps. The first step is the development of a steel sheet to be used in the shallow floor slab with the determination of the geometry, dimensions and materials. The second one comprises the bending tests of the slab models for evaluation of their behavior. In the first stage, an overall research on composite slabs used in several countries in Europe and North America was made due to the lack of research on steel sheets for this purpose in Brazil.

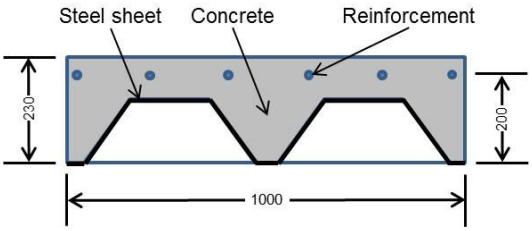

Fig. 4 Cross section of the slab models (unit: millimeters)

Based on this research, geometry similar to these existing sheets in these countries was defined.

The experimental program consisted of 6 models of composite steel and concrete slabs subjected to four-point bending test. The models were divided into two groups: group 1 with 3000 mm of span and 1000 mm of width (Fig. 3(a)) and group 2 with span of 1500 mm and 1000 mm of width (Fig. 3(b)). Tests for the characterization of the materials (concrete and steel sheet) were carried out.

Each group of slabs consisted of three models: one model tested with monotonic load and two models with two stages of testing. In the first stage the models were subjected to a cyclic load with five thousand cycles, and the second stage the models were subjected to a monotonic load till failure. Table 1 summarizes the models dimensions, their groups and the tests that they were subjected.

The slab models had total height equal to 230 mm and reinforcement cover with 30 mm as specified by Brazilian Code ABNT NBR 6118 (2003). According to that same code, in order to combat the effects of shrinkage and temperature, the slab should have reinforcement in its top with the ratio of 0.1% of the area of concrete between the top and the steel sheet, as shown in Fig. 4.

As previously mentioned, the steel sheet was specially manufactured for the construction of models due to there is no equivalent sheet suitable for shallow floors commercialized in Brazil. The manufacturing steps were: First steel plates were cut off in sheets with dimensions of 2.00 m × 3.00 m. These sheets were cold folded to form the ribs. Finally, with the use of a press, dents were printed one by one on the sides of the ribs. Fig. 5 presents the dimensions of the ribs.

According to Ferrer *et al.* (2006), the inclination of dents is one of the most important parameters face to the shear strength. Degrees variation can cause large variations in strength. Another important point is the depth of the dents.

In Ferrer *et al.* (2006) an increase of 1.5 mm to 3 mm in the depth of the dents increased three times the strength.

The dents of the steel sheet produced had a depth of 2 to 2.5 mm (Fig. 6).

Fig. 6 Dents of the steel sheet

Fig. 7 Cracking inducer

The tests were performed in accordance with EUROCODE 4 (2004). As recommended by this code, a cracking inducer was done in the local of load application, as shown in Fig. 7. The cracking inducer becomes the weak section and ensures that the failure by shearing occurs at this point. In the case of two load points, the shear span is the distance from the center of support to the nearest loading point.

2.2 Instrumentation

The instrumentation of the slab models consisted of strain gages and displacement transducers (LVDT). The displacement transducers were used to determine the end slip (Fig. 8(a)) and also to measure the deflection below the slab (Fig. 8(b)). Displacement transducers with 100mm long were used for measuring the deflection and with 50mm long for measuring the end slip.

Two types of strain gages were used to measure the strains, the KGF - 5-120 - C1 – 11 and KFG - 10 - 120 - C1 - 11. The first one was used for steel elements and the

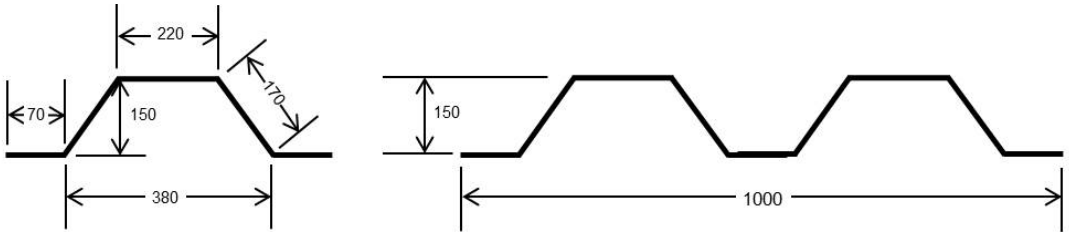

Fig. 5 Dimensions of the steel sheet (unit: millimeters)

(a) End slip

(b) Deflection

Fig. 8 Positions of the displacement transducers

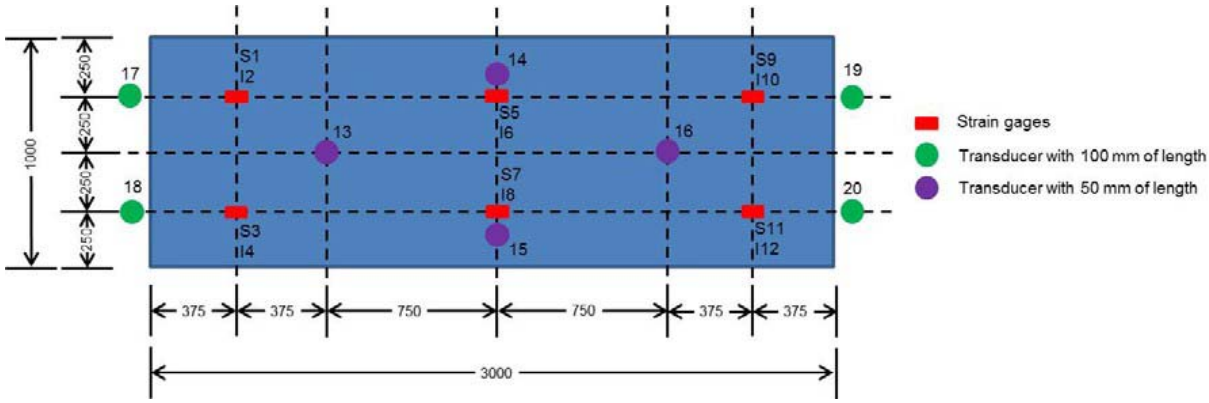

Fig. 9 Instrumentation of the models of group 1 (unit: millimeters)

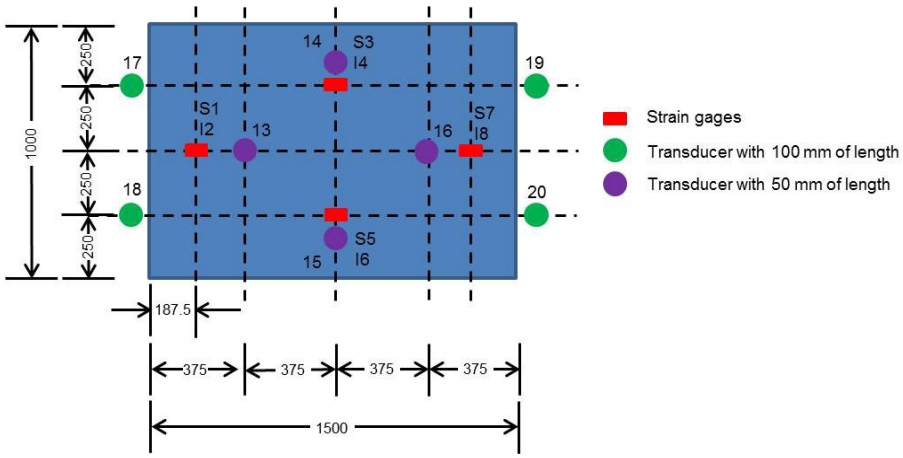

Fig. 10 Instrumentation of the models of group 2 (unit: millimeters)

Fig. 11 Test setup of model 1 of group 1

second for concrete elements. Figs. 9 and 10 present the position of the strain gauges and the displacement transducers for groups 1 and 2. The strain gages in concrete are indicated by letter "S" and in the steel sheet by letter "I". Instrumentation points indicated by a circle are displacement transducers.

2.3 Test setup

As Brazilian Code do not have prescriptions for slim floor test, the recommendations of EUROCODE 4 (2004) were adopted. At first time a model of each group of slabs

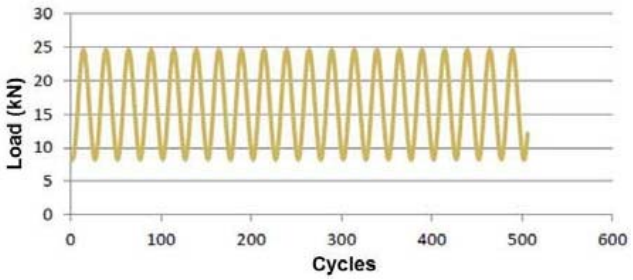

Fig. 12 Load × cycles curve

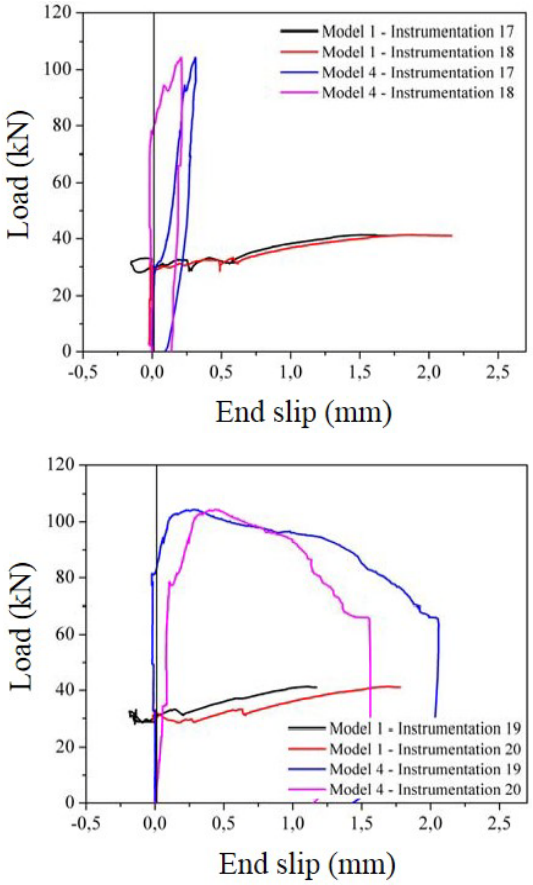

Fig. 13 Load × end slip curves – Model 1 × Model 4

was tested to monotonic loading with displacement control, as can be seen in Fig. 11. Models subjected to monotonic loading were model 1 of group 1 and model 4 of group 2.

The others two models of each group were subjected to two stages of loading. In the first phase the slab models were subjected to a cyclic loading with 5000 cycles. The cyclic loading had the load ranged from 20 to 60 percent of the tensile strength of the model tested with monotonic loading; it was carried out to break the chemical bond. In the second phase, the models were subjected to monotonic loading till failure.

The intensity of the loading cycles varied between 8.24 kN and 24.72 kN, as shown in Fig. 12. The considered loading failure is the maximum load applied plus the own weight of the model and the weight of the steel beam used to apply the loading.

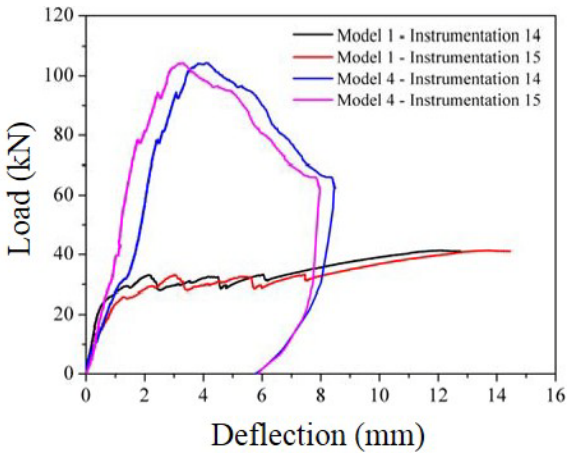

Fig. 14 Load × deflection in mid-span curves – Model 1 × Model 4

3. Experimental results

3.1 Analysis of the influence of the span

For the analysis of the influence of the span length in the behavior of the shallow floor slab, the load *versus* end slip curves and load *versus* mid-span deflection curves were compared.

The comparison was carried out between models with the same type of loading. That means that model 1 was compared to model 4 and models 2 and 3 were compared to models 5 and 6.

3.1.1 Model 1 × Model 4 - Load × end slip curves

Models 1 and 4 were subjected only to monotonic loading to allow an individual analysis of the influence of the slab span. Fig. 13 presents the load *versus* end slip curves.

As expected, the slab model with 1500 mm of length (model 4) presented the maximum load higher than model 1. It was observed that the maximum load had an increase markedly of 152%. The results showed that the strength of this type of slab is not proportional to the span.

Taking the end slip into account, the behavior of model 4 was different considering their sides, while model 1 presented almost the same behavior in both sides. For model 4 the relative displacement concentrated in one side with 2 mm of slippage, in other side just 0.25 mm were observed. Such behavior was also expected, due to the difference of the span length.

3.1.2 Model 1 × Model 4 - Load x deflection curves

Analyzing the load *versus* mid-span deflection curves for models 1 and 4 presented in Fig. 14, it was possible to conclude that these models presented the same initial stiffness, however, the span had no influence on this parameter.

It was also noted in the behavior of model 1 that a gain of strength after the initial slippage happened. In model 4 such occurrence was not observed, due to after the load peak, the load came down. It means that model 1 had a ductile behavior compared to model 4.

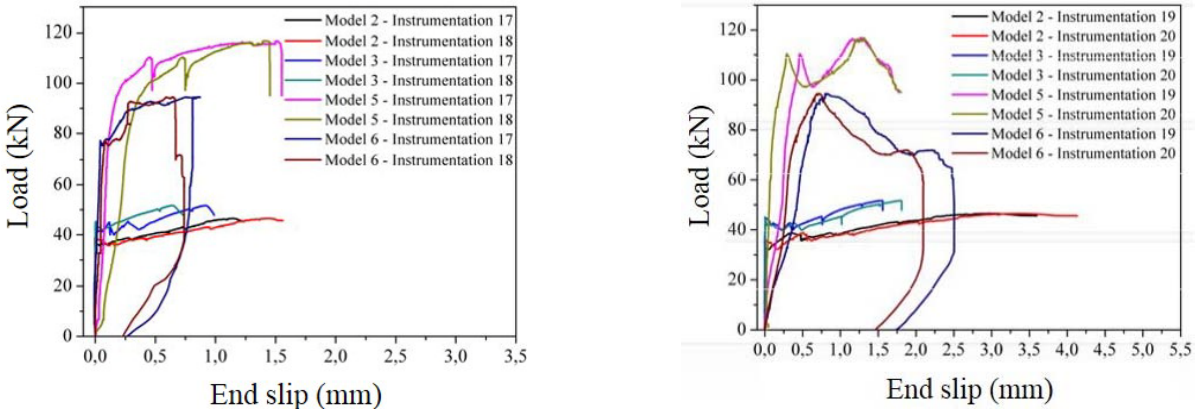

Fig. 15 Load × end slip curves – Models 2 e 3 × Models 5 e 6

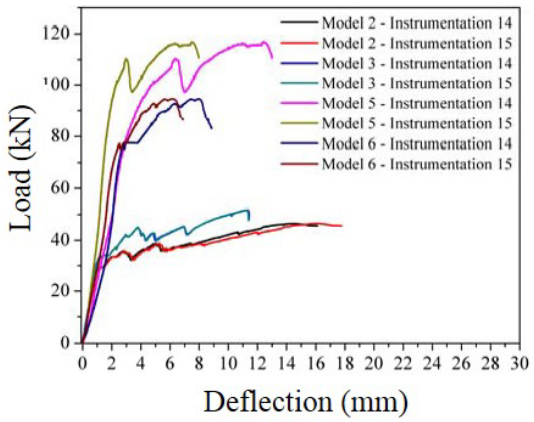

Fig. 16 Load × deflection in mid-span curves – Models 2 e 3 × Models 5 e 6

3.1.3 Model 2 and Model 3 × Model 5 and Model 6 - Load × end slip curves

Fig. 15 provides the load *versus* end slip curves for monotonic loading of the models of group 1 and group 2, which were previously subjected to cyclic loading. The end slip of the slabs of group 1 were closer to zero during almost the test. On the other hand, the slab models of group 2 presented end slip since the beginning of the test. That observation indicates that for models with smaller span the chemical bond was broken, and the cyclic test accomplished his goal, which was not observed in group 1. As already observed in the comparison between models 1 and 4, the gain of strength occurred after the first slippage for models 2 and 3.

The behavior observed in model 4 (model just tested subjected to monotonic loading) was also presented by models 5 and 6. A brittle behavior was observed for models with 1500 mm long and a ductile behavior for models with 3000 mm long.

3.1.4 Model 2 and Model 3 × Model 5 and Model 6 - Load × deflection in mid-span curves

Overall, the models 2, 3, 5 and 6 presented similar initial stiffness till 30 kN of load. At maximum load, the instrumentation point number 14 belonging to model 5 presented more higher deflection in mid-span than other models due to the prematurely disruption of adhesion between the steel sheet and the concrete (Fig. 16).

3.2 Comparison between the behaviors of slab models that belonging to the same group

3.2.1 Group 1 - Load × end slip curves

Regarding to the relative displacement of group 1, it was expected that model 1 reached higher load due to it was not subjected to cyclic loading. This result was not observed in the experimental tests, models 2 and 3 presented higher

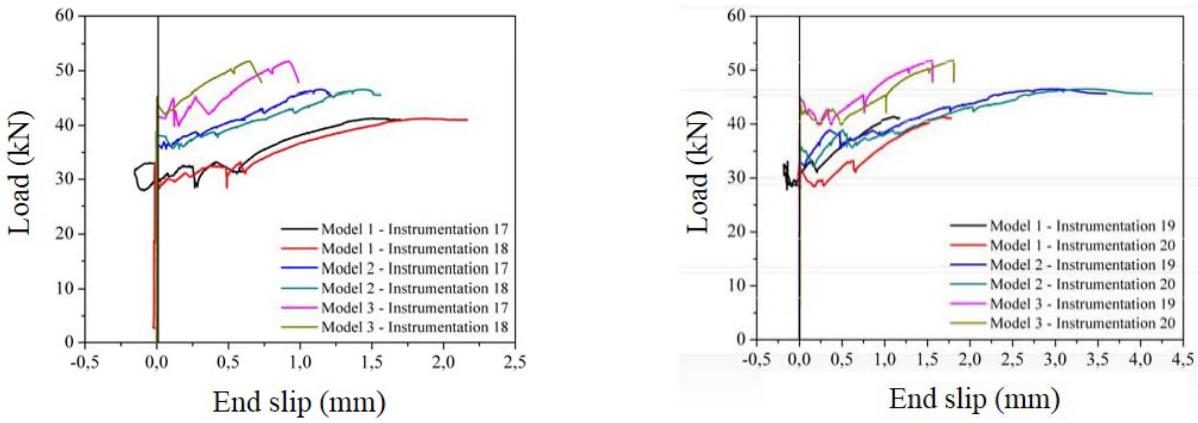

Fig. 17 Load × end slip curves – Group 1

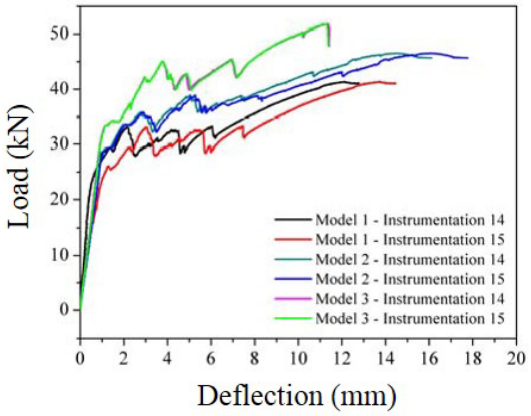

Fig. 18 Load × deflection in mid-span curves – Group 1

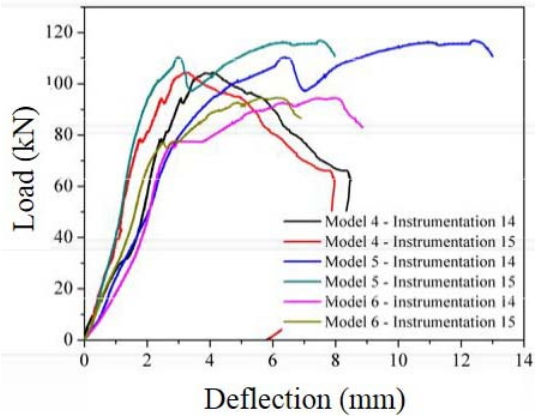

Fig. 20 Load × deflection in mid-span curves – Group 2

maximum load (Fig. 17). There are two reasons for these results: the chemical bond was not broken in the cyclic test or problems occurred during the construction of model 1. Some aspects observed in the results were in accordance with expectations. For model 1, the moment that the chemical bond was broken is evident because of the presence of a level and a next the gain of strength occurs due to mechanical interlock.

3.2.2 Group 1 - Load × deflection in mid-span curves

According to the load *versus* deflection in mid-span curves shown in Fig. 18, the slab models of group 1 presented similar behavior. The initial stiffness was the same for all the models and this result confirms the hypothesis that the cyclic test did not broken completely the chemical bond. Analyzing the behavior of model 3, the same conclusion can be done; it was the slab that presented higher maximum load, contradicting the expectations.

3.2.3 Group 2 - Load × end slip curves

Fig. 19 presents the load *versus* end slip curves obtained from tests of the models of group 2. Unlike the slab models of group 1, the slabs with smaller span belonging to group 2 had the chemical bond broken by cyclic test. This result is evidenced by the difference between the initial stiffness due to the models with chemical bond broken presented stiffness lower than the slab model with intact bond (model 4).

The curves related to the displacement transducers number 17 and 18 of model 5 showed where the mechanical interlock is broken. This instant corresponds to the point where the curve presents a drop with subsequent increase, as observed by Widjaja (1997).

It was also observed a level in the load *versus* end slip curves of models 5 and 6, with constant slippage. However, this level is small when it is compared to the models of group 1 due to the absence of the chemical bond. Such behavior is not observed in model 4, which presented a brittle failure. It seems possible that the brittle failure is consequence the disruption of the chemical bond and the mechanical interlock has occurred at the same time.

3.2.4 Group 2 - Load x deflection in mid-span curves

Models of group 2, which were previously subjected to cyclic test, presented initial stiffness lower than model 4, according to load *versus* deflection in mid-span curves, shown in Fig. 20. As mentioned before, model 4 presented brittle failure and models 5 and 6 had a ductile behavior because they presented higher displacement till failure.

The results of vertical displacement in mid-span also validate the conclusion that the models subjected to cyclic load of group 2 had the chemical bond broken in the first stage because of their initial stiffness.

3.3 Steel sheet strains

In the bending tests of the slabs, the strains of the steel

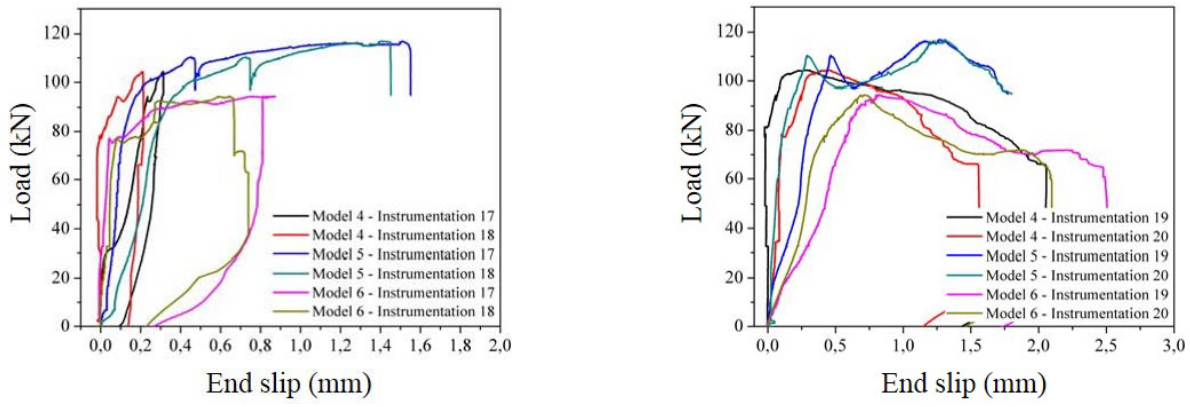

Fig. 19 Load × end slip curves – Group 2

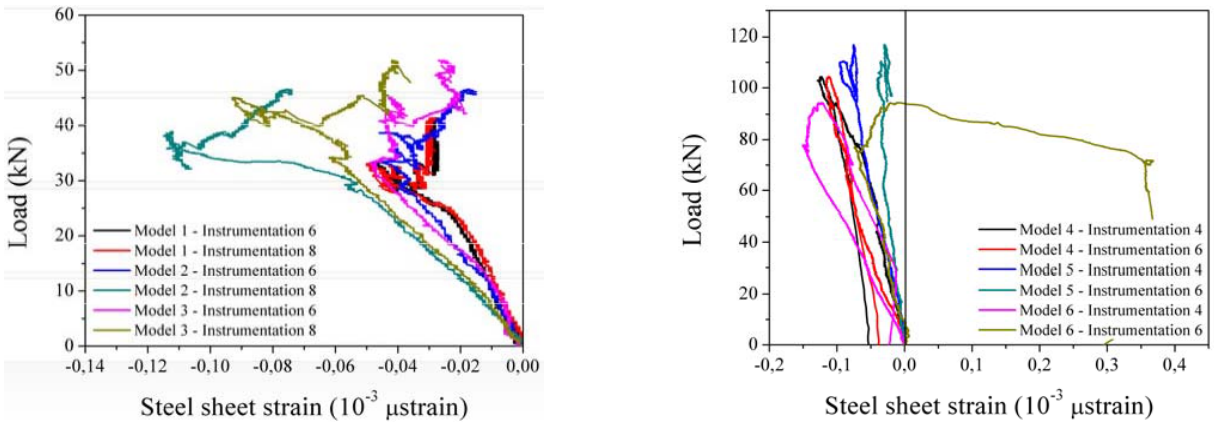

(a) Group 1 (b) Group 2

Fig. 21 Load × Strains in the steel sheet curves

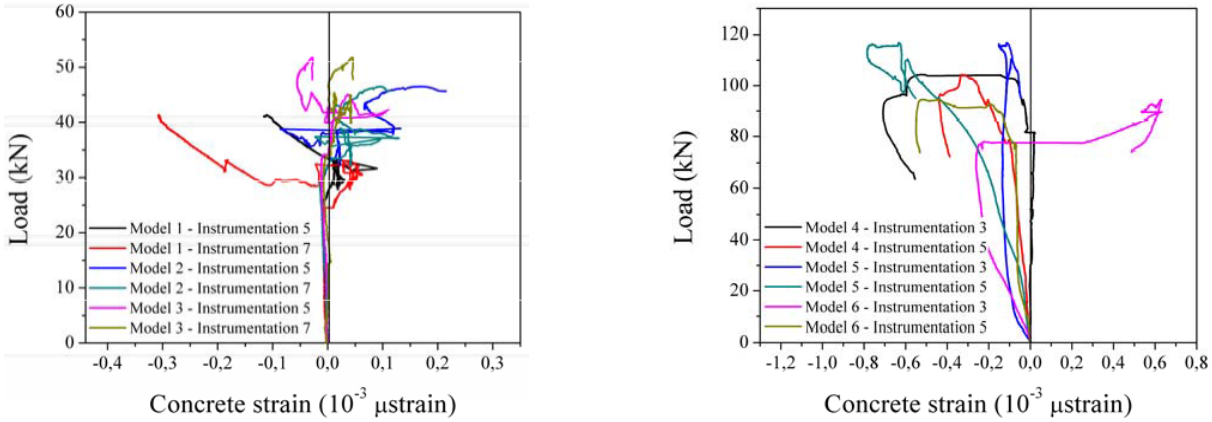

(a) Group 1 (b) Group 2

Fig. 22 Load × Strains in concrete curves

sheets were measured with strain gages. Load *versus* strain curves for models of groups 1 and 2 are presented in Fig. 21. The behavior of the steel sheets, as already concluded in previous analysis, allows saying that models of group 1 presented ductile behavior, characterized by higher deformation of the steel sheet. Overall, all the readings of strains showed negative values, which indicate compression stresses in the steel sheet. This result is justified by the local where the strain gages were placed, at the top of the ribs of the steel sheet. In the beginning of the tests, the top of the ribs is requested by compressive stresses, and the neutral axis is placed in the middle of the slab cross section.

During the test, the strains by compressive stresses began to decrease and the steel sheet starts to be required by tensile stresses. This result probably happened due to upward movement of the neutral axis, and at those points the chemical bond still existed, the system started working with compression stresses in the concrete and tensile stresses in the steel. However, this chemical bond breaks down quickly, and the ribs come back to be required by compressive stresses.

3.4 Concrete strains

The concrete strain was measured on the top surface of the slab models. As expected, the concrete was compressed during almost all the time of the bending test. For the both groups of slabs, the strains measured presented similar values. In the beginning of the test, the concrete was compressed and with the opening of cracks, some disturbances occur as well as tensile stresses. Fig. 22 provides the load *versus* strains in concrete curves for models of group 1 and group 2.

3.5 Comparison between experimental and theoretical results

For the comparisons between the experimental and theoretical results, the sizing of the slabs was carried out according to prescriptions of Brazilian Code ABNT NBR 8800 (2008) and EUROCODE 4 (2004). The objective of this comparison is to correlate the experimental values with the theoretical results in order to assess if the tests were consistent. In that analysis the failure mode was identified, remembering that in the experimental tests was the longitudinal shear.

The moment and shear diagrams to the experimental results are presented in Fig. 23 for models of group 1 and Fig. 24 for models of group 2. The diagrams were drawn considering only the maximum load obtained in the tests of

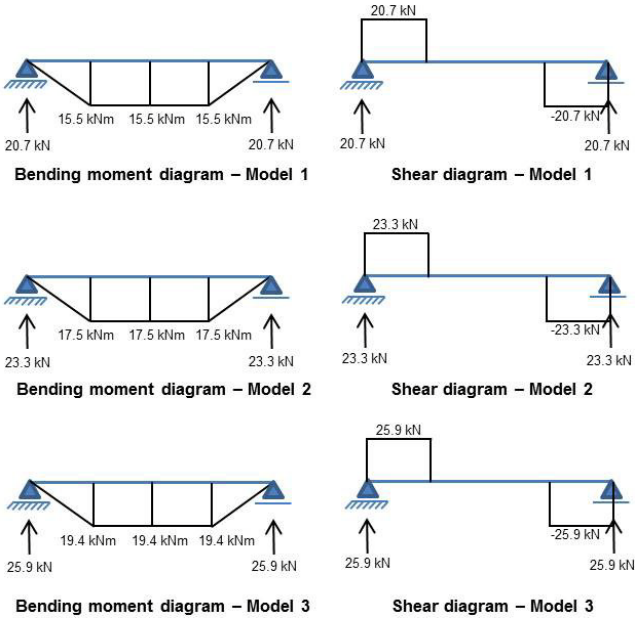

Fig. 23 Moment and shear diagrams of the experimental results – Group 1

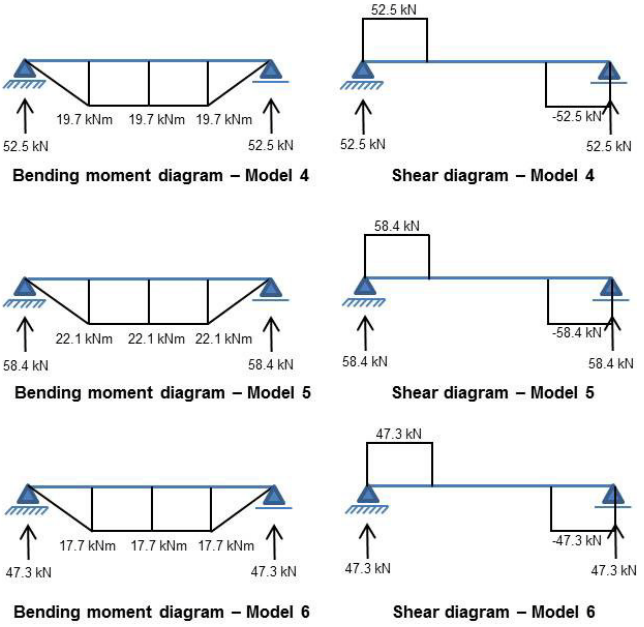

Fig. 23 Moment and shear diagrams of the experimental results – Group 1

each slab model and did not take the own weight of the slab into account as well as the weight of the steel beams used to apply the loading.

The bending moment resistant obtained by the slabs sizing (theoretical value) were determined considering the neutral axis above the sheet profile (Fig. 25). To calculate the maximum bending moment resistant it was used the equations 1 to 4, and the shear force (Vthe) was determine based on it, considering the test arrangement (Fig. 26) and equation 5. The experimental (Vexp) and theoretical (Vthe) values of shear are provided in Table 2.

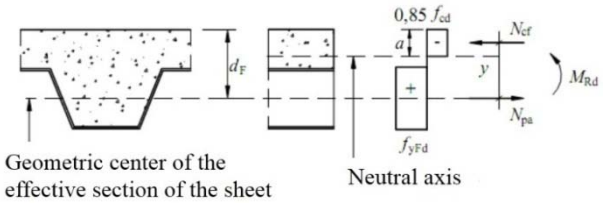

Fig. 25 Stress diagram for positive bending moment (neutral axis above the steel sheet)

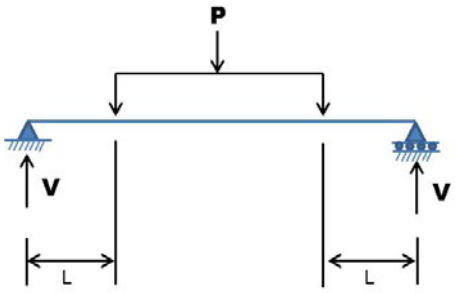

Fig. 26 Arrangement of the tests

$$M_{Rd} = N_{pa}\,(d_f - 0{,}5a) \tag{1}$$

$$N_{pa} = A_{F,ef}\,.\,f_{yFd} \tag{2}$$

$$a = \frac{N_{pa}}{0{,}85\,.\,f_{cd}\,.\,b} \tag{3}$$

$$y = h_t - 0{,}5t_c - e_p + (e_p - e)\frac{N_{cf}}{N_{pa}} \tag{4}$$

Where:

$A_{F,ef}$ is the area of the profiled sheet section.

f_{yFd} is the characteristic yield strength of the steel sheet.

d_f is the distance from the upper face of the concrete slab to the geometric center of the effective section of the sheet;

b is the width of the slab

f_{cd} is the characteristic compressive strength of the concrete.

e is the distance from the centroid of the effective area of the sheet to its underside.

e_p is the distance from the plastic neutral axis of the effective area of the sheet to its underside.

According to the comparison, the obtained theoretical values (Vthe) of shear were higher than the experimental values (Vexp), demonstrating that the procedure of sizing prescribed by Brazilian Code and international code are not in favor of safety. The shear results of the experimental models of group 2 were closer to theoretical values than Group 1. These results can be consequence of the interface area that changes the behavior of the slab; the interface area of group 1 is bigger than the interface of group 2 and because of that its behavior became more distant from the theoretical result.

$$M_{max} = \frac{V_{the}\,.\,L}{8} \tag{5}$$

Table 2 Experimental and theoretical values of shear force

Group	Model	V_{exp} (kN)	V_{the} (kN)	V_{exp}/V_{the}	% deviation
1	Model 1	20.70	29.40	0.70	30
	Model 2	23.30		0.79	21
	Model 3	25.90		0.88	12
2	Model 4	52.50	58.81	0.89	11
	Model 5	58.40		0.99	1
	Model 6	47.30		0.80	20

4. Analyzes and discussions

The tests results showed that the failure mode of the six slab models was by longitudinal shear. The load *versus* end slip curves and the load *versus* deflection described satisfactorily the behavior of the system, allowing to identify the longitudinal shear as the predominant failure mode. For all models, it was observed in the load *versus* end slip curves a level or a decrease in the load before a gain of strength. According to Widjaja (1997), in small-scale tests, this point indicate that the mechanical interlock provided by the dents in the steel sheet is over, and from that point the thickness of the sheet and the height of the rib will guarantee the resistance and stiffness.

The failure by longitudinal shear is considered by several researchers as the governing mode of failure of the composite slabs, due to it is difficult to ensure the total interaction between steel sheet and concrete, then it limits the strength of this element. However, the sizing predicted by Brazilian code assumes that the section has complete interaction, therefore, for the system to reach the bending moment determined in the calculation, the longitudinal shear strength should be increased. It was observed in some slabs that, next to reach the maximum load, the chemical adhesion in the top table of the sheet began to present tensile stresses; as the interaction present in this region was partial, the slab failed and did not reach the moment resistant determine in calculation.

The models of group 2 had the chemical adhesion broke by the cyclic tests, observation proved by the initial stiffness of the monotonic bending test due to model 4 presented higher stiffness than models 5 and 6. Regarding to group 1, the chemical adhesion was only weakened, probably because the size of the interface area. However, the models of group 2 had brittle behavior and they reached higher maximum load than the models of group 2, which presented a ductile behavior.

Regarding to the new steel sheet developed in this research, the experimental results showed that this element behaved as expected, demonstrating a considerable resistance to longitudinal shear, which was comprised by chemical adhesion between and mechanical interlock. This assertion is verified because the longitudinal shear was only 16% (average) lower than the theoretical one.

5. Conclusions

According to the experimental results, the novel steel sheet behaved as expected, presenting satisfactory longitudinal shear strength, provided by natural adhesion (chemical bond) and the mechanical interlock.

For models with shear span equal to 325 mm (group 2), the cyclic tests broke the chemical bond, but the models with shear span of 700 mm (Group 1) long, the chemical bond was only weakened, probably because the area of the interface is twice than the area of the smaller model. However, the models of group 2 had brittle failure and the models of group one had ductile behavior.

In the beginning of the tests, it was observed that the slab models had the neutral axis in the middle of the cross section of the steel sheet, which was not considered in the design. Calculations admitted the section working with full interaction, so that for the system reached the strength determined in the calculus of the bending moment resistant, the longitudinal shear strength should be improved. Next to failure load, in some slab models, it was observed that the chemical bond in the top of the steel sheet presented tensile stresses. Due to the partial interaction, the slab broke and the maximum strength determined in the calculation of the bending moment was not reached.

Overall, the characteristics adopted for the steel sheet such as the geometry and the position of the dents provided a good performance regarding to the shear strength of composite floor slabs. The results of the study confirmed that the developed sheet is suitable for use in composite slabs without damage to the global behavior of the structure.

Acknowledgments

The authors would like to thank FAPESP for the financial support and also the Laboratory of Structures of the University of São Paulo by performing the tests.

References

Abdullah, R. (2004), "Experimental evaluation and analytical modeling of shear bond in composite slabs", M.A.Sc. Dissertation; Virginia Polytech Institute, Blacksburg, VA, USA.

ABNT - Brazilian Association of Technical Codes (2003), NBR 6118: Design of reinforced concrete structures: Procedure, Rio de Janeiro, Brazil, 170 p. [In Portuguese]

ABNT - Brazilian Association of Technical Codes (2008), NBR 8800: Design and execution of steel concrete composite building structures: Procedures, Rio de Janeiro, Brazil, 237 p. [In Portuguese]

Al-Deen, S., Ranzi, G. and Uy, B. (2015), "Non-uniform shrinkage in simply-supported composite steel- concrete slabs", *Steel Compos. Struct., Int. J.*, **18**(2), 375-394.

Chen, S. and Shi, X. (2011), "Shear bond mechanism of composite slabs - A universal FE approach", *J. Construct. Steel Res.*, **67**(10), 1475-1484.

Chen, S., Limazie, T. and Tan, J. (2015), "Flexural behavior of shallow cellular composite floor beams with innovative shear connections", *J. Construct. Steel Res.*, **106**, 329-346.

Daniels, B. and Crisinel, M. (1988), "Composite slab with profiled shetting", *Proceedings of an Engineering Foudation Conference on Compostie Construction in Steel and Concrete*, *ASCE*, Henniker, NH, USA, June, pp. 656-662.

De Nardin, S. and El Debs, A.L.H.C. (2009), "Study of partially

encased composite beams with innovative position of stud bolts", *J. Construct. Steel Res.*, **65**(2), 342-350.
De Nardin, S. and El Debs, A.L.H.C. (2011), "Composite connections in slim-floor system: An experimental study", *J. Construct. Steel Res.*, **68**(1), 78-88.
Easterling, W.S. and Young, C.S. (1992), "Strength of composite slabs", *J. Struct. Eng., ASCE*, **118**(9), 2370-2389.
EUROCODE 4 (2004), Design of composite steel and concrete structures – Part 1-1: General rules and rules for buildings, European Committee for Standardization.
Ferrer, M., Marimon, F. and Crisinel, M. (2006), "Designing cold-formed steel sheets for composite slabs: An experimentally validated FEM approach to slip failure mechanics", *Thin-Wall. Struct.*, **44**(12), 1261-1271.
Friedrich, J.T. (2012), "Experimental and theorical analysis of composite shallow floors", Master Dissertation; School of Engineering of São Carlos, University of São Paulo, São Carlos, Brazil, 128 p. [In Portuguese]
Huo, B.Y. and D'Mello, C.A. (2013), "Push-out tests and analytical study of shear transfer mechanisms in composite shallow cellular floor beams", *J. Construct. Steel Res.*, **88**, 191-205.
Johnson, R.P. (1994), *Composite Structures of Steel and Concrete, Beams, Columns, Frames and Applications in Buildings*, (Vol. 1), Blackwell Scientific Publications, London, UK.
Kataoka, M.N. and El Debs, A.L.H.C. (2013), "Modelo de elementos finitos para análise não linear de piso misto de pequena altura", *IX Congresso de Construção Metálica e Mista I Congresso Luso-Brasileiro de Construção Metálica Sustentável*, Porto, Portugal. [In Portuguese]
Kataoka, M.N. and El Debs, A.L.H.C. (2014), "Parametric study of composite beam-column connections using 3D finite element modeling", *J. Construct. Steel Res.*, **102**, 136-149.
Kataoka, M.N. and El Debs, A.L.H.C. (2015), "Beam–column composite connections under cyclic loading: An experimental study", *Mater. Struct.*, **48**(4), 929-946.
Kim, H.Y. and Jeong, Y.J. (2010), "Ultimate strength of a steel-concrete composite bridge deck slab with profiled sheeting", *Eng. Struct.*, **32**(2), 534-546.
Marimuthu, V., Seetharaman, S., Arul Jayachandran, S., Chellappan, A., Bandyopadhyay, T.K. and Datta, D. (2007), "Experimental studies on composite deck slabs to determine the shear-bond characteristic (m-k) values of the embossed profile sheet", *J. Construct. Steel Res.*, **63**(6), 791- 803.
Salonikios, T.N., Sextos, A.G. and Kappos, A.J. (2012), "Tests on composite slabs and evaluation of relevant Eurocode 4 provisions", *Steel Compos. Struct., Int. J.*, **13**(6), 571-586.
Saravanan, M., Marimuthu, V., Prabha, P., Arul Jayachandran, S. and Datta, D. (2012), "Experimental investigations on composite slabs to evaluate longitudinal shear strength", *Steel Compos. Struct., Int. J.*, **13**(5), 489-500.
Shen, G. (2001), "Perfomance evaluation of new corrugated-type embossments for composite deck", M.A.Sc. Thesis.
Seleim, S. and Schuster, R. (1985), "Shear-bond resistance of composite deck-slabs", *Can. J. Civil Eng.*, National Research Council of Canada, **12**(2), 316-324.
Vainiünas, P., Valivonis, J., Marciukaitis, G. and Jonaitis, B. (2006), "Analysis of longitudinal shear behaviour for composite steel and concrete slabs", *J. Construct. Steel Res.*, **62**(12), 1264-1269.
Widjaja, R.B. (1997), "Analysis and design of steel deck – Concrete composite slabs", Master Dissertation; Faculty of the Virginia Polytechnic, Blacksburg, VA, USA.